Polyoxometalates

DOI: 10.1002/anie.201404621

Exploring the Symmetry, Structure, and Self-Assembly Mechanism of a Gigantic Seven-Fold Symmetric $\{Pd_{84}\}$ Wheel**

*Rachel A. Scullion, Andrew J. Surman, Feng Xu, Jennifer S. Mathieson, De-Liang Long, Fadi Haso, Tianbo Liu, and Leroy Cronin**

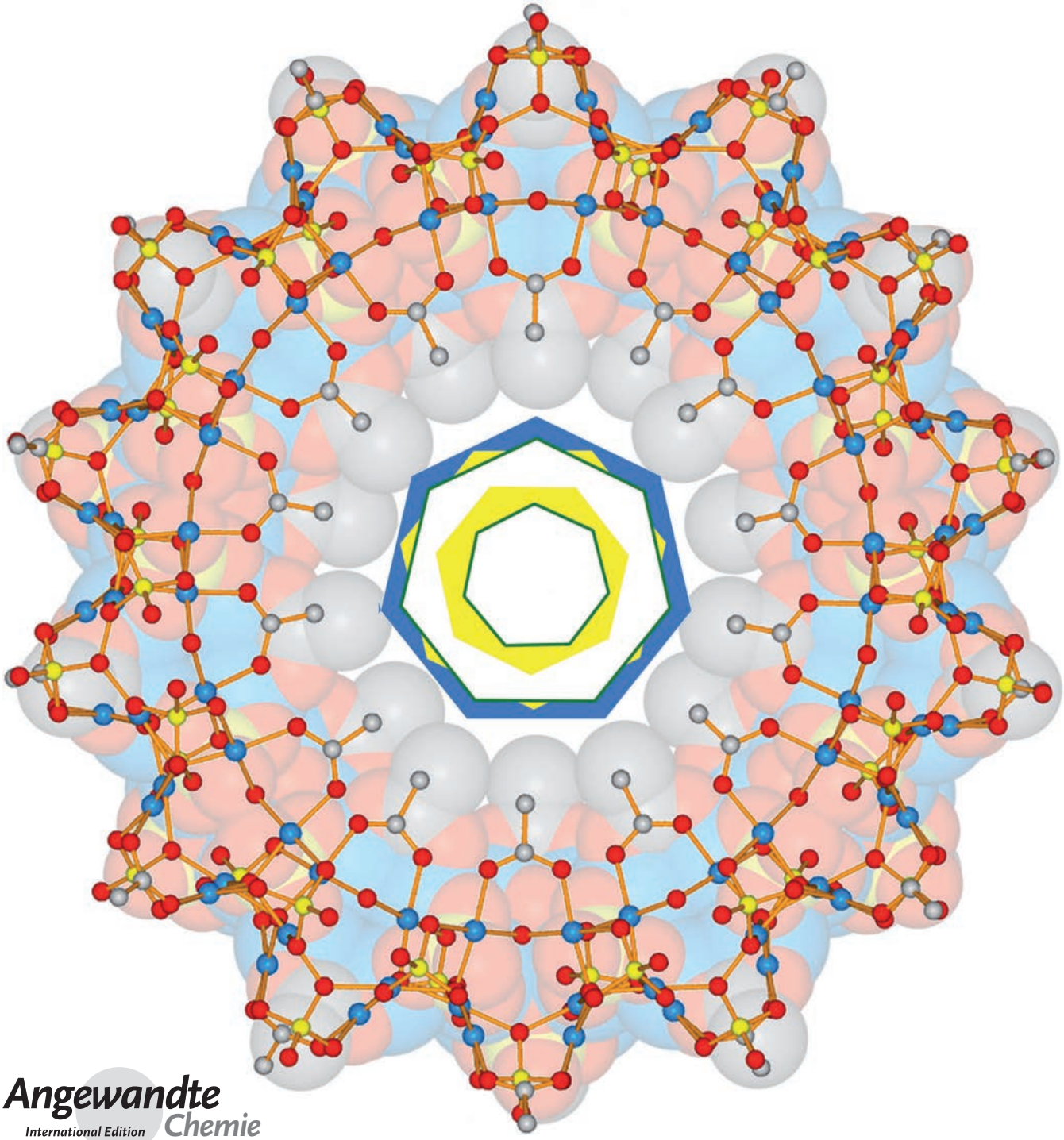

Abstract: *The symmetry, structure and formation mechanism of the structurally self-complementary* ***{Pd$_{84}$}*** *= [Pd$_{84}$O$_{42}$(PO$_4$)$_{42}$(CH$_3$CO$_2$)$_{28}$]$^{70-}$ wheel is explored. Not only does the symmetry give rise to a non-closest packed structure, the mechanism of the wheel formation is proposed to depend on the delicate balance between reaction conditions. We achieve the resolution of gigantic polyoxopalladate species through electrophoresis and size-exclusion chromatography, the latter has been used in conjunction with electrospray mass spectrometry to probe the formation of the ring, which was found to proceed by the stepwise aggregation of {Pd$_6$}$^-$ = [Pd$_6$O$_4$(CH$_3$CO$_2$)$_2$(PO$_4$)$_3$Na$_{6-n}$H$_n$]$^-$ building blocks. Furthermore, the higher-order assembly of these clusters into hollow blackberry structures of around 50 nm has been observed using dynamic and static light scattering.*

Polyoxometalates (POMs)[1] are polynuclear clusters of transition metals (mainly Mo, W, and V) with a massive range of nuclearity from 6 to 368 metal atoms in a single cluster.[2] The assembly of POM-based giant molecular wheels for example, {Mo$_{154}$}[3] or {Mo$_{176}$},[4] is especially striking and in particular it is interesting to compare the family of POM Mo wheels with the wheels reported by Winpenny et al.,[5] in terms of symmetry, structure, and lability. The assembly of the gigantic wheel {Mn$_{84}$} cluster with 6-fold symmetry showed that giant ring-shaped clusters were possible outside of Mo-based POMs,[6] although it is not yet clear what principles govern the assembly of these gigantic wheel nanostructures. When low-nuclearity POMs of Pt, Au, and Pd (POPd) were reported we wondered if this family was limited to smaller clusters or if it could be extended to large wheel assemblies.[7] Recently we discovered the largest polyoxopalladate to date[8]—a **{Pd$_{84}$}** wheel with the formula [Pd$_{84}$O$_{42}$(PO$_4$)$_{42}$(CH$_3$CO$_2$)$_{28}$]$^{70-}$, an overall diameter of 3 nm, a core of around 1 nm, and a molecular weight greater than 16 kDa. Remarkably, although this huge cluster could be synthesized in a simple one-pot reaction comprising two reagents giving crystals in less than two weeks, it appeared that the assembly process is highly complicated. Understanding the process would be all but impossible due to the combinatorial complexity associated with the number of configurations and the possible molecular structure/fragment state space. The key question is how could a ring as large as **{Pd$_{84}$}** spontaneously form and crystallize within the period of days. Indeed the state space for the molecule, just considering the unique arrangements of the 84 Pd atoms gives a combinatorial space of $84! = 3.3 \times 10^{126}$.

Herein, we show that it is possible to follow the stepwise assembly of palladate clusters in solution, culminating in the formation of the **{Pd$_{84}$}** wheel, by using a combination of techniques including electrophoresis and size exclusion chromatography (SEC), as well as high resolution mass spectrometry as a function of time. The combination of the data obtained from these techniques allows us to postulate a reaction mechanism for **{Pd$_{84}$}** as well as discuss how slight changes in the reaction conditions impact the formation of smaller clusters, namely [H$_7$Pd$_{15}$O$_{10}$(PO$_4$)$_{10}$]$^{13-}$ = **{Pd$_{15}$}** and the previously unpublished neutral cluster, [Pd$_{10}$O$_4$(CH$_3$CO$_2$)$_{12}$(H$_2$O)$_2$] = **{Pd$_{10}$}**.

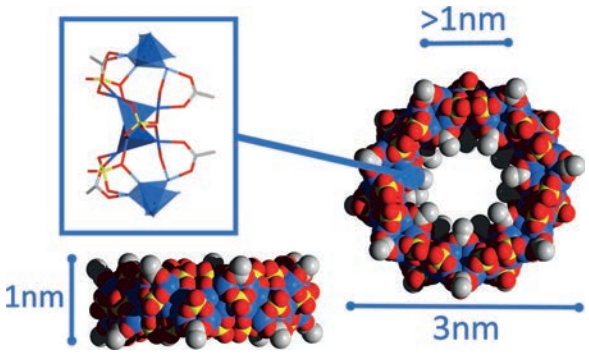

Figure 1. Space filling model of **{Pd$_{84}$}** showing the front and side views. The inset shows a {Pd$_6$O$_2$}$_2$ subunit which is linked through two bridging acetate, one bridging phosphate and a μ_2-oxo ligand. Colors: Pd blue, P yellow, O red, C gray.

The ring, shown in Figure 1, comprises seven {[Pd$_6$(μ_4-O)$_2$(μ_2-O)(CH$_3$CO$_2$)$_2$(PO$_4$)$_3$]$_2$} units ({Pd$_6$O$_2$}$_2$) with D_{7d} symmetry and a C_7 (S_{14}) axis. In each of these minimal {Pd$_6$O$_2$} repeating units, all 6 palladium ions are connected through two unusual μ_4-O ligands. The 14 {Pd$_6$O$_2$} subunits are directly linked to each other by μ_2-O ligands and neighboring subunits are bridged by four acetate and two phosphate ligands. Half of the acetate ligands are found in the cavity of the wheel resulting in a hydrophobic core, with the remaining 14 located around the outside of the wheel. The phosphate ligands are either capping (2 per {Pd$_6$O$_2$} subunit) or bridging between adjacent subunits. The former results in the surface of the molecule being hydrophilic and both types contribute to the high water solubility of the compound overall.

One feature of the crystal packing of **{Pd$_{84}$}** is that it has 7-fold symmetry, and we are interested if the symmetry, structure and mechanism are linked. This is because, according to Kitaigorodskii's principle of close packing,[9] maintain-

[*] R. A. Scullion, Dr. A. J. Surman,[+] Dr. J. S. Mathieson,[+] Dr. D.-L. Long, Prof. L. Cronin
WestCHEM, School of Chemistry, University of Glasgow
University Avenue, Glasgow G12 8QQ (UK)
E-mail: lee.cronin@glasgow.ac.uk
Homepage: http://www.croninlab.com
Dr. F. Xu[+]
State Key Lab of Chemo/Bio Sensing
College of Science and Engineering, Hunan Univeristy
Changsha, 410082 (PR China)
F. Haso, Prof. T. Liu
Department of Polymer Science, University of Akron
Akron, OH 44325 (USA)
[+] These authors contributed equally to this work.

[**] We thank the EPSRC, WestCHEM, and the University of Glasgow for supporting this work as well as Shodex for lending us several columns.

Supporting information for this article (experimental details including the synthesis of **{Pd$_{84}$}**, **{Pd$_{15}$}**, and **{Pd$_{10}$}** along with electrophoresis, SEC-HPLC, and time-resolved mass spectrometry data as well as their detailed assignment) is available on the WWW under http://dx.doi.org/10.1002/anie.201404621.

ing void space within the crystal lattice is always unfavorable. Consequently, orders of symmetry with a prime number greater than or equal to 5 are disfavored. Therefore, with its higher order of symmetry of 7, the crystallization of {**Pd$_{84}$**} should be unfavorable, yet this is the major species that crystallizes after 10 days despite having 7-fold symmetry, forming tubes with the acetates displaced one seventh of a turn on the wheel down the *a* axis (Figure 2).

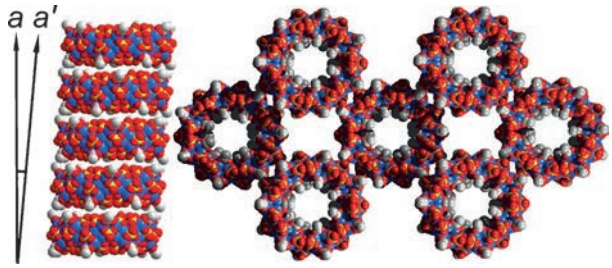

Figure 2. Crystal packing of {**Pd$_{84}$**} viewed parallel to the *a* axis showing the wheels "locked" together in tubes down the *a* axis (left) and from above the *bc* plane with the tubes "locked" together in the plane (right). Each {**Pd$_{84}$**} cluster is surrounded by four closest adjacent clusters at the plane [100], revealing a non-closest packing pattern; the deviation from the *a* and the ring "tube" propagation axis "*a*" is evident as well as the "locking" interactions.

Thus, the formation of the structure, despite the lack of close packing, appears to be dominated by the molecular self-complementarity between the wheels arising whereby the acetate CH_3 groups can interdigitate between adjacent wheels up and down the nanotubes, and in the planes, where each cluster is surrounded by eight other clusters, and hence does not adopt a closest packing arrangement, again due to the complementary "locking" interactions. Viewed along the crystallographic *a* axis, the crystal packing indicates its tendency to form layer networks parallel to the *bc* plane. However, when viewed along the crystallographic *c* axis, the unusual symmetry is expressed noticeably by the clear tilt between the rotation axis of each molecular plane and the crystal lattice, which leads to the formation of a compromised "curved plane". The regularity of the tubular stacks formed in the crystal packing, along with the increased volume conferred to the materials from the non-closest packing arrangement should mean that {**Pd$_{84}$**} is highly interesting. This is because the 7-fold symmetry structure appears to be a highly selected product from a vast state space.

To investigate this idea, we set about exploring the synthesis of the {**Pd$_{84}$**} wheel in solution. $Pd(OAc)_2$ is added to a buffered phosphate solution within the pH range of 6.5–7.1 and the suspension is stirred at room temperature for around 20 h. After about 10 days, the product can be isolated in ca. 20% yield based on palladium. By doing in the region of 1000 experiments, we have been able to map the effect of both temperature and pH on the formation of {**Pd$_{84}$**}. The former is most evident when compared to the synthetic procedure for {**Pd$_{15}$**}. Specifically, if the reaction is carried out at room temperature, {**Pd$_{84}$**} was found to be the main product formed. However, if the temperature is increased to 85 °C for as little as 90 min, {**Pd$_{15}$**} will be the major product. Similarly, if the pH of crystallization during the synthesis of {**Pd$_{84}$**} is less than 4.5, red precipitate forms which, after recrystallization in methanol, can be identified as a neutral decanuclear complex, $[Pd_{10}(CH_3COO)_{12}O_4(H_2O)_2]$ ({**Pd$_{10}$**}) (Figure 3). Time-resolved mass spectrometry studies show that a {**Pd$_{10}$**}$^-$ species, of formula $[Pd_{10}O_4(CH_3CO_2)_{13}]^-$, can be observed in {**Pd$_{84}$**} mother liquor from the first day of crystallization

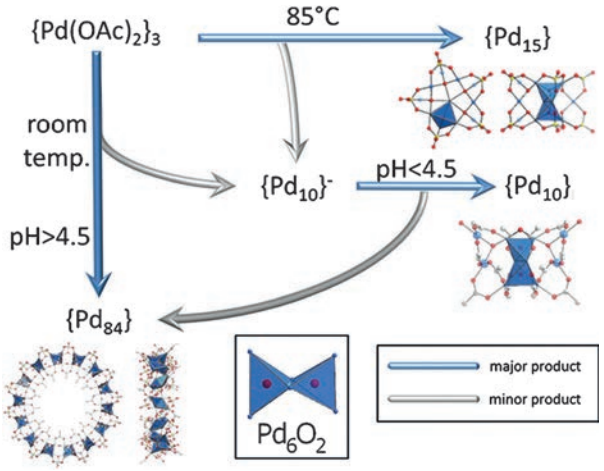

Figure 3. Proposed assembly process of POPds in aqueous solution with the $\{Pd_6O_2\}$ unit highlighted in each of the structures. The different reaction conditions required for each of the species to be the main product are also shown. Colors: Pd blue, P yellow, O red, C gray, $\{Pd_6O_2\}$ units blue tetrahedra.

until day eleven when crystals of the ring form (see Supporting Information (SI), Figure S1). The absolute intensity of the {**Pd$_{10}$**}$^-$ peak decreases in the first few days suggesting the formation of other species in the mother liquor. We propose that, in the reaction solution, a $\{Pd_6O_2\}$ core is initially formed from the palladium acetate trimer in the buffer solution in the form of the incipient {**Pd$_{10}$**}$^-$ species. If the pH is lower than 4.5, the mono-protonated {**Pd$_{10}$**} cluster forms irreversibly due to its poor solubility in aqueous solution. The hydrophobicity of this cluster can be attributed to the presence of methyl groups projecting from the surface of the molecule in all directions. If the pH is higher than 4.5, on the other hand, the {**Pd$_{10}$**}$^-$ species remains in solution with {**Pd$_{84}$**} being the main product.

Due to the complex mixture of products and salts in the reaction mixture, direct analysis by conventional means is unsuitable. For example, in electrospray mass spectrometry (ESI-MS) high buffer/salt concentrations leads to both suppression of signals associated with the cluster and obscuring signals resulting from salt clustering. New tools were therefore required to characterize the species forming in solution. Gel electrophoresis (GE) has previously been shown by our group to be a useful tool to resolve POM mixtures based on their differing electrophoretic mobilities, which are a function of both the size and charge of the species.[10] By modifying the previously reported technique, it was possible to resolve {**Pd$_{84}$**} and {**Pd$_{15}$**} species from a mixture of pure

solutions of both components. This was observed as the distinctively colored {**Pd$_{15}$**} band moving toward the anode faster than that of {**Pd$_{84}$**}. However, the same analysis of {**Pd$_{84}$**} mother liquor did not separate into well-defined bands and instead produced a poorly-defined streak (see SI Figure S2). This indicates a wide range of species of various sizes and charges are present in the mother liquor, but does not resolve them or give much information on their nature, and this again points to the crystallization process "selecting" one possible cluster from a plethora of possibilities.

Size-exclusion chromatography (SEC) is a technique used to separate solution species based solely on their size, regardless of their chemistry (charge, hydrophobicity etc.). Like GE, it is widely used in biochemistry for both preparative and analytical separations; however we are not aware of its application to POM chemistry. To investigate its potential, we attempted to resolve {**Pd$_{84}$**} and {**Pd$_{15}$**} from a 1:1 mixture of both using a standard polymer-based SEC column eluting 0.05 M sodium acetate buffer at pH 5 (for full experimental details, see SI). Having optimized the conditions, two large peaks were observed, almost completely resolved as can be seen in the top section of Figure 4. These

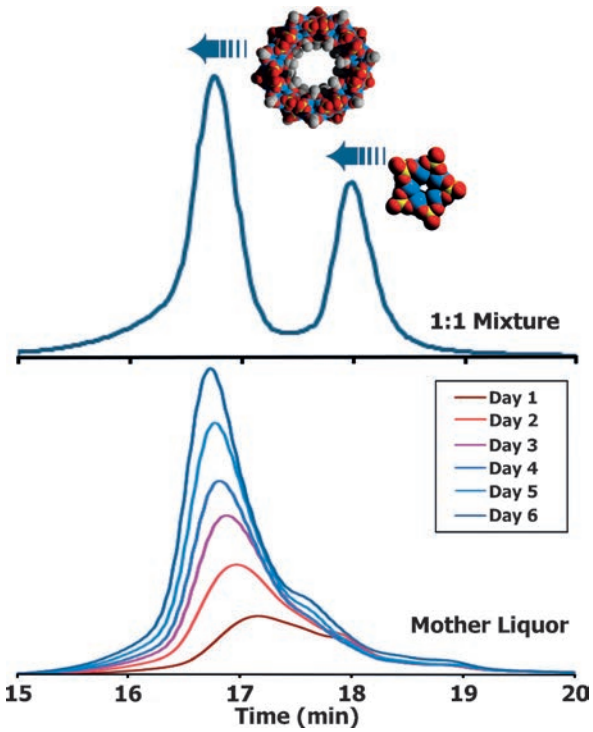

Figure 4. Bottom: SEC-HPLC trace of {**Pd$_{84}$**} mother liquor over the course of six days. Top: The separation of a 1:1 mixture of mixed solutions composed from individually dissolving pure crystalline samples of {**Pd$_{84}$**} and {**Pd$_{15}$**} compounds.

were confirmed to correspond to {**Pd$_{84}$**} (16.7 min) and {**Pd$_{15}$**} (18 min) by comparison with pure solutions. As expected, this corresponds to elution of species ordered by size and demonstrates SEC as a tool to observe the relative size of POMs.

Having established this methodology, it was then applied to {**Pd$_{84}$**} mother liquor to observe the change in size of species present over time (bottom half of Figure 4). On day one, the mother liquor shows a very broad peak after 17 min that corresponds to species of sizes between {**Pd$_{15}$**} and {**Pd$_{84}$**}. Over the course of six days, this peak sharpens and shifts to a maximum at 16.7 min, matching exactly the retention time of {**Pd$_{84}$**}. To ensure that the change in retention time was not due to error within the instrument between runs, a solution of {**Pd$_{84}$**} crystals was run and the retention time compared to that of the previous day; no drift was observed. This progression indicates the growth of larger species in solution with time, culminating with the formation of {**Pd$_{84}$**}.

Although this SEC approach shows the progressive growth of species in the reaction solution, it does not identify them. ESI-MS, on the other hand, has been frequently used to follow POM formation,[11] but cannot be directly applied to the mother liquors in this study. In biological systems, which have analogous ion suppression issues, SEC is often used to "de-salt" samples prior to ESI-MS analysis. To investigate this combination with our system, aliquots of {**Pd$_{84}$**} mother liquor were initially desalted using small disposable size-exclusion "spin columns" (MicroBioSpin 6) before ESI-MS analysis. This yielded spectra in which large anions consistent with the {**Pd$_{84}$**} species could be observed, however, due to the molecular cut off of the spin columns, smaller species such as {**Pd$_{15}$**} were not. To remedy this, the analytical SEC column used for observing the growth of species in mother liquor was coupled to an ESI-MS instrument (SEC-MS), with water as eluent in place of buffer. Again, a 1:1 mixture of {**Pd$_{84}$**} and {**Pd$_{15}$**} solutions was run as a test and the resulting chromatogram showed a loss of resolution due to the low ionic strength of the eluent. However, the species were eluted in a similar time range and the mass spectra obtained were of a high quality. As this was also the case with {**Pd$_{84}$**} mother liquor, a time-resolved study of the mother liquor was performed. From day one, several low nuclearity Pd fragments could be observed. A peak at *m/z* 1100, which is prevalent throughout the whole study, was tentatively assigned as $[Pd_6O_4(CH_3CO_2)_2(PO_4)_3Na_{(6-n)}H_n]^-$ ($\{Pd_6\}^-$). It is worthwhile to note that all other identifiable species could be assigned as resulting from species incorporating multiples of the $\{Pd_6\}^-$ "building block". For example, on day one, dimer $\{Pd_{12}\}^{3-}$, pentamer $\{Pd_{30}\}^{4-}$ and hexamer $\{Pd_{36}\}^{5-}$ species could be identified (see SI Section 7 for full assignments). On subsequent days (days two to five), a larger $\{Pd_{48}\}^{6-}$ species can be seen and the intensity of all other $\{Pd_6\}$-derived fragments increases with time. By day six, peaks consistent with those observed on elution of a {**Pd$_{84}$**} solution are first detected (in 9−, 10− and 11− charged states). We can also identify fragments that can be assigned as resulting from $\{Pd_{66}\}^{9-}$ and $\{Pd_{78}\}^{10-}$. With the exception of $\{Pd_6\}^-$ and $\{Pd_{12}\}^{3-}$, all of the other smaller fragments are no longer identifiable in the mass spectrum by day six. Remarkably, we can observe an overall increase in charge in the sample over the course of the six days, as shown in Figure 5. This indicates the formation of large, highly charged species in solution. We propose this is due to the assembly of the $\{Pd_6\}^-$ building blocks into larger fragments with a higher charge, which then combine to form

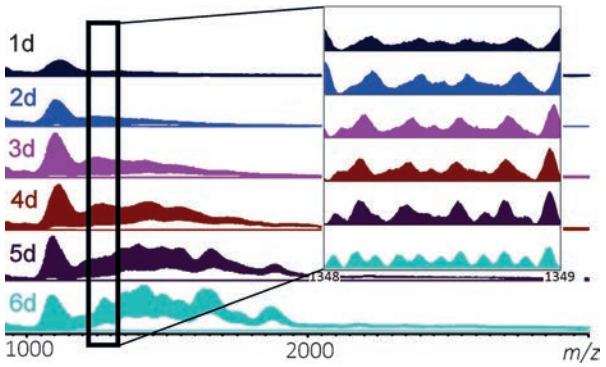

Figure 5. Time-resolved mass spectra of {$\mathbf{Pd_{84}}$} mother liquor after SEC-HPLC in water focusing on the region 1000–2000 *m/z*. Inset shows the increase in charge of species in the same area over the course of six days. The peak at *m/z* 1100 has been tentatively assigned as the building block, $[Pd_6O_4(CH_3CO_2)_2(PO_4)_3Na_{(6-n)}H_n]^-$.

the wheel. The aggregation of species in solution is limited by the curvature of these $\{Pd_6\}^-$ units resulting in the termination of growth at the {$\mathbf{Pd_{84}}$} wheel.

Having investigated how the wheel forms in solution, its higher-order assembly behavior in water was monitored using dynamic and static light scattering (DLS and SLS) along with transmission electron microscopy (TEM). This macro-ion carries a moderate amount of charge on its surface making it suitable to overcome electrostatic repulsion and self-assemble into hollow spherical blackberry-like structures. The time-resolved scattering intensity plot suggests a mechanism that is consistent with super colloid cluster of clusters "blackberry" formation,[12] that is the presence of a lag phase in the early days where individual {$\mathbf{Pd_{84}}$} clusters form oligomers, the increase of the scattering intensity that corresponds to overcoming the activation energy barrier for blackberry formation, and the stabilization at higher intensity suggesting the formation of blackberries. CONTIN analysis[13] of the DLS measurement shows that the blackberries that form in water (0.2 mg mL^{-1} {$\mathbf{Pd_{84}}$}) have an average hydrodynamic radius (R_h) of 52 nm, which is close to the radius of gyration (R_g) obtained from SLS (54 nm) indicating the existence of hollow spherical assemblies. The size of the blackberry-like assemblies remains unchanged during the self-assembly process (see SI), indicating that smaller blackberry structures are not present in the system as intermediate species (this is also consistent with our previous study[14]). Furthermore, images obtained from TEM suggest the presence of the blackberries with sizes that are consistent with the light scattering results (Figure 6).

In summary, we have probed the self-assembly of a gigantic cluster using a combination of techniques including electrophoresis, size-exclusion chromatography (SEC) and combined SEC with ESI-MS to analyze the components of the mother liquor as a function of time. This approach has yielded the first insight in to how the giant {$\mathbf{Pd_{84}}$} wheel forms in solution. Consequently, we have tentatively assigned $\{Pd_6\}^-$ as the building block for the formation of {$\mathbf{Pd_{84}}$} by aggregation over the course of several days. This suggests that the ring forms from multiples of $\{Pd_6\}$ to give 14 as a possible magic number ($6 \times 14 = 84$ and $14! = 8.7 \times 10^{10}$) and a much more manageable state space.

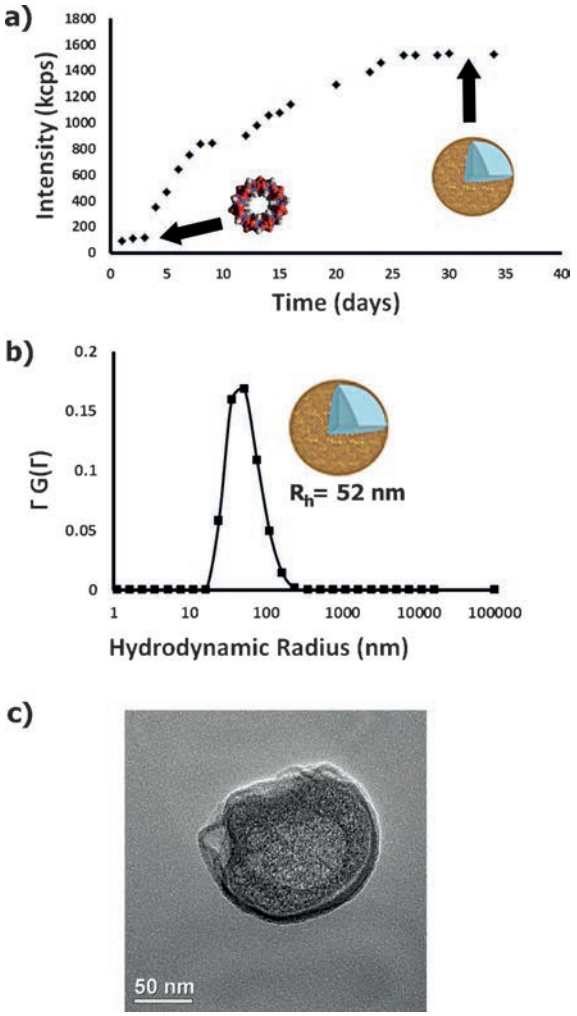

Figure 6. a) Time-resolved scattering intensity curve showing the blackberry formation process. b) CONTIN analysis of the DLS measurements showing that the assemblies having a radius of 52 nm. c) TEM image showing blackberries of {$\mathbf{Pd_{84}}$} having a size that is consistent with the DLS measurements.

Experimental Section

CCDC 846615 ({$\mathbf{Pd_{84}}$}) and 998507 ({$\mathbf{Pd_{10}}$}) contain the supplementary crystallographic data for this paper. These data can be obtained free of charge from The Cambridge Crystallographic Data Centre via www.ccdc.cam.ac.uk/data_request/cif.

Received: April 23, 2014
Published online: July 9, 2014

Keywords: palladium · polyoxometalates · size-exclusion chromatography · self-assembly

[1] D.-L. Long, R. Tsunashima, L. Cronin, *Angew. Chem.* **2010**, *122*, 1780–1803; *Angew. Chem. Int. Ed.* **2010**, *49*, 1736–1758.

[2] A. Müller, E. Beckmann, H. Bögge, M. Schmidtmann, A. Dress, *Angew. Chem.* **2002**, *114*, 1210 – 1215; *Angew. Chem. Int. Ed.* **2002**, *41*, 1162 – 1167.
[3] A. Müller, E. Krickemeyer, J. Meyer, H. Bögge, F. Peters, W. Plass, E. Diemann, S. Dillinger, F. Nonnenbruch, M. Randerath, C. Menke, *Angew. Chem.* **1995**, *107*, 2293 – 2295; *Angew. Chem. Int. Ed. Engl.* **1995**, *34*, 2122 – 2124.
[4] A. Müller, E. Krickemeyer, H. Bögge, M. Schmidtmann, C. Beugholt, P. Kögerler, C. Lu, *Angew. Chem.* **1998**, *110*, 1278 – 1281; *Angew. Chem. Int. Ed.* **1998**, *37*, 1220 – 1223.
[5] a) A. J. Blake, C. M. Grant, S. Parsons, J. M. Rawson, R. E. P. Winpenny, *J. Chem. Soc. Chem. Commun.* **1994**, 2363 – 2364; b) F. K. Larsen, E. J. L. McInnes, H. E. Mkami, J. Overgaard, S. Piligkos, G. Rajaraman, E. Rentschler, A. A. Smith, G. M. Smith, V. Boote, M. Jennings, G. A. Timco, R. E. P. Winpenny, *Angew. Chem.* **2003**, *115*, 105 – 109; *Angew. Chem. Int. Ed.* **2003**, *42*, 101 – 105.
[6] A. J. Tasiopoulos, A. Vinslava, W. Wernsdorfer, K. A. Abboud, G. Christou, *Angew. Chem.* **2004**, *116*, 2169 – 2173; *Angew. Chem. Int. Ed.* **2004**, *43*, 2117 – 2121.
[7] a) M. Pley, M. S. Wickleder, *Angew. Chem.* **2004**, *116*, 4262 – 4264; *Angew. Chem. Int. Ed.* **2004**, *43*, 4168 – 4170; b) N. V. Izarova, N. Vankova, T. Heine, R. N. Biboum, B. Keita, L. Nadjo, U. Kortz, *Angew. Chem.* **2010**, *122*, 1930 – 1933; *Angew. Chem. Int. Ed.* **2010**, *49*, 1886 – 1889; c) E. V. Chubarova, M. H. Dickman, B. Keita, L. Nadjo, F. Miserque, M. Mifsud, I. W. C. E. Arends, U. Kortz, *Angew. Chem.* **2008**, *120*, 9685 – 9689; *Angew. Chem. Int. Ed.* **2008**, *47*, 9542 – 9546; d) Y. Xiang, N. V. Izarova, F. Schinle, O. Hampe, B. Keita, U. Kortz, *Chem. Commun.* **2012**, *48*, 9849 – 9851.
[8] F. Xu, H. N. Miras, R. A. Scullion, D.-L. Long, J. Thiel, L. Cronin, *Proc. Natl. Acad. Sci. USA* **2012**, *109*, 11609 – 11612.
[9] A. I. Kitaigorodskii, *Organic chemical crystallography*, Consultants Bureau, New York, **1961**.
[10] R. Tsunashima, C. Richmond, L. Cronin, *Chem. Sci.* **2012**, *3*, 343 – 348.
[11] H. N. Miras, E. F. Wilson, L. Cronin, *Chem. Commun.* **2009**, 1297 – 1311.
[12] T. Liu, E. Diemannm, H. Li, A. W. M. Dress, A. Müller, *Nature* **2003**, *426*, 59 – 62.
[13] S. W. Provencher, *Comput. Phys. Commun.* **1982**, *27*, 229 – 242.
[14] T. Liu, *J. Am. Chem. Soc.* **2003**, *125*, 312 – 313.

